1 **Title**

2 **Modelling cancer immunomodulation using epithelial organoid cultures**

3

4 **Authors**

5 Yotam E. Bar-Ephraim[1,2,8], Kai Kretzschmar[1,2,8], Priyanca Asra[1,2], Evelien de Jongh[1,2], Kim E.

6 Boonekamp[1,2], Jarno Drost[3], Joost van Gorp[4], Apollo Pronk[5], Niels Smakman[5], Inez J. Gan[6],

7 Zsolt Sebestyén[6], Jürgen Kuball[6], Robert G.J. Vries[7], Hans Clevers[1,2,3*]

8

9 [1]Oncode Institute, Hubrecht Institute, Royal Netherlands Academy for Arts and Sciences

10 (KNAW) and University Medical Centre (UMC) Utrecht, the Netherlands

11 [2]UMC Utrecht, Cancer Genomics Netherlands, Utrecht, the Netherlands

12 [3]Princess Máxima Centre for Paediatric Oncology, Utrecht, the Netherlands

13 [4]Department of Pathology, Diakonessenhuis hospital, Utrecht, the Netherlands

14 [5]Department of Surgery, Diakonessenhuis hospital, Utrecht, the Netherlands

15 [6]Laboratory of Translational Immunology, Department of Immunology, UMC, Utrecht, the

16 Netherlands

17 [7]Foundation Hubrecht Organoid Technology (HUB), Utrecht, the Netherlands

18 [8]These authors contributed equally: Yotam E. Bar-Ephraim, Kai Kretzschmar

19

20 *Corresponding author, e-mail: h.clevers@hubrecht.eu

21

22 **Here we utilize organoid technology to study immune-cancer interactions and assess**

23 **immunomodulation by colorectal cancer (CRC). Transcriptional profiling and flow**

24 **cytometry revealed that organoids maintain differential expression of**

25 **immunomodulatory molecules present in primary tumours. Finally, we established a**

26 **method to model antigen-specific epithelial cell killing and cancer immunomodulation in**

27 **vitro using CRC organoids co-cultured with cytotoxic T cells (CTLs).**

28

29 CRC is among the most common cancers worldwide[1]. While early CRC stages are highly

30 treatable by surgical removal, later stages are usually incurable[2]. CRC arises through a multi-

31 step process from small lesions of the epithelium of the large intestine. These lesions grow into

32 adenomas with low grade dysplasia that progress into high grade dysplasia, eventually giving

33 rise to infiltrating carcinomas[3]. Genetic mutations in signalling pathways such as the canonical

34 Wnt signalling are the molecular basis of CRC[4]. However, the interaction of the tumour with

35   its microenvironment is another critical hallmark[5]. Cancer cells remodel their

36   microenvironment (e.g. fibroblasts, the vasculature and immune cells) to support tumour

37   growth[6]. Infiltrating immune cells (ICs) such as CTLs or macrophages play a crucial role by

38   generating different immune responses such as anti-tumour cytotoxicity (the former) or

39   tumour-promoting chronic inflammation (the latter)[7]. As such, escape from the surveilling

40   immune system has been recognised as one of the hallmarks of cancer[5]. Cancer cells undergo

41   a process called immunoediting and silence anti-tumour responses, for example, by preventing

42   T-cell activation through stimulation of inhibitory cell surface receptors such as CTL-

43   associated antigen (CTLA)-4 or programmed death (PD)1[6,8]. Overcoming this active

44   immunomodulation by tumour cells has become a major therapeutic target[9]. However, tumour

45   heterogeneity, such as differential CTL infiltration or differential expression of immune

46   inhibiting factors, could influence therapeutic efficiency of anti-tumour drugs by mediating

47   drug resistance[6]. Developing *ex vivo* model systems to characterise the communication of the

48   tumour with its environment is therefore of great importance. Organoid cultures grown from

49   different epithelial tissues serve as an excellent tool to study tissue homeostasis and disease[10].

50   Furthermore, organoid biobanks of multiple epithelial organ systems have been established and

51   tumour-derived organoids have successfully been used as platforms for screenings of different

52   drugs to predict patient response[11]. Here we describe the establishment of a method to model

53   antigen-specific epithelial-cell killing and cancer immunomodulation and *in vitro* using CRC

54   organoids co-cultured with CTLs.

55

56   We first assessed whether CRC organoids expressed immunomodulatory molecules in

57   established long-term expanded cultures. To this end, we compared gene expression of T-cell-

58   specific immunomodulators in CRC organoids to the expression levels found in normal colon

59   organoids using a transcriptome dataset generated using our 'living organoid biobank' of CRC

60   patients[12]. On average, transcription of genes associated with T-cell stimulation such as

61   *TNFSF4* or *TNFSF9* was not altered in CRC organoids compared to normal colon organoids

62   (Fig. 1a). However, expression of human leukocyte antigen (HLA) genes *HLA-A* and *HLA-C*,

63   encoding major histocompatibility complex class (MHC)-I molecules that present antigens to

64   T cells, were significantly downregulated in CRC organoids (Fig. 1a), a well-described

65   phenomenon found in cancers[13]. Expression of genes associated with inhibition of T-cell

66   function was either significantly upregulated such as *BTLA*, significantly downregulated such

67   as *CD80*, *CD86* or LGALS9 or not altered at all such as *CD274* (encoding PD-L1),

68   *PDCD1LG2* (encoding PD-L2) (Fig. 1a). When assessing expression levels of

2

69   immunomodulatory molecules on individual organoids, CRC organoids largely clustered

70   together showing heterogeneous down regulation of *HLA-A*, *HLA-C* and *LGALS9* compared to

71   healthy colon organoids (Fig. 1b). However, expression of immunoinhibitory genes *CD274*

72   and *PDCD1LG2*, for instance, was highly upregulated in some CRC organoids in comparison

73   to the matched normal colon organoid cultures, reflecting previously reported preservation of

74   tumour heterogeneity in organoids[12] (Fig. 1b). These molecular signatures provide a basis for

75   further investigation of tumour immunogenicity and its association with other characteristics

76   of the tumour.

77   Four of the most commonly mutated genes in CRC are *APC*, *P53*, *KRAS* and *SMAD4*,

78   reflecting the stepwise progression of the normal intestinal epithelium into a metastatic

79   carcinoma[14]. Introduction of these cancer mutations into human intestinal organoid cultures

80   using clustered regularly interspaced short palindromic repeats (CRISPR)/Cas9 demonstrated

81   that this process can be mimicked *in vitro* and upon xenotransplantation into mice[15,16]. Using

82   colon organoids carrying one or more of these cancer mutations, we investigated whether up-

83   regulation of PD-L1 was associated with a certain mutational status. Additionally, we exposed

84   mutant organoids and their wild-type control organoid line to interferon (IFN)-γ, which is

85   secreted by T cells and can trigger increased expression of immunomodulatory molecules such

86   as PD-L1[17]. Subsequently, we assessed PD-L1 expression by quantitative polymerase chain

87   reaction (qPCR) and flow cytometry (Fig. 1 c,d). In the absence of IFN-γ, organoids carrying

88   triple ($APC^{KO/KO}$, $P53^{KO/KO}$, $KRAS^{G12D/+}$) and quadruple mutations ($APC^{KO/KO}$, $P53^{KO/KO}$,

89    $KRAS^{G12D/+}$ and $SMAD4^{KO/KO}$) showed lower *CD274* gene expression in comparison to control

90   wild-type organoids (Fig. 1 c). Overall, PD-L1 expression was low in untreated organoid lines

91   (Fig. 1 c,d). However, PD-L1 expression was dramatically upregulated in IFN-γ-treated

92   organoids both on transcript and protein level (Fig. 1 c,d). These data demonstrate that CRC

93   organoids express immunomodulators and that this expression is regulated in a similar way as

94   previously shown for tissue *in vivo*.

95

96   We next aimed at establishing a co-culture system for CRC organoids and CTLs to model

97   antigen-specific killing of tumour cells *in vitro*. For this, we used $\alpha\beta$ T cells carrying a

98   transgenic T-cell receptor (TCR) recognizing an HLA-A2-restricted Wilms tumour (WT)1-

99   derived peptide[18,19]. We first screened CRC organoids from the 'living biobank'[12] as well as

100   newly generated CRC organoids for HLA-A2 expression using flow cytometry. We found

101   three CRC organoid lines that showed partial downregulation of HLA-A2 (Supplementary Fig.

102 1a). We were able to purify HLA-A2$^+$ and HLA-A2$^-$ CRC organoids and successfully

103 established cultures from both populations (Fig. 2b). We confirmed stable MHC-I

104 downregulation in HLA-A2$^-$ CRC organoids, as IFN-γ stimulation did not trigger HLA-A2 re-

105 expression (Supplementary Fig. 1b). Next, we pulsed these CRC organoid lines with WT1

106 peptide and, subsequently, co-cultured them for 48 hours with peptide-specific T cells.

107 Following co-culture, we found that HLA-A2$^-$ CRC organoids did survive irrespective of

108 whether pulsed with the peptide or not (Fig. 2c). However, only the HLA-A2$^+$ CRC organoids

109 without prior peptide incubation survived co-culture (Fig. 2c). Peptide-pulsed HLA-A2$^+$ CRC

110 organoids were effectively killed by the peptide-specific T cells providing a proof-of-principle

111 that organoids can be utilised to study anti-tumour response by cytotoxic T cells *in vitro*.

112   To further confirm antigen-specificity in our 'killing' assay system, we improved our

113 co-culture method by transfecting HLA-A2$^+$ CRC organoids with a construct expressing

114 mNeonGreen-tagged histone H2B and staining T cells with CellTracker violet to allow for

115 long-term tracking of both cell types (Methods). We then pulsed HLA-A2$^+$ CRC organoids

116 with either the WT1 peptide or with an EBV-derived peptide (Methods) and co-cultured the

117 organoids with T cells carrying either a WT1- or an EBV-specific TCR. Here, only organoids

118 pulsed with the cognate peptide were efficiently killed by the T cells (Fig. 2d, Supplementary

119 Movies 1 and 2). Testing for IFN-γ production by the T cells in the co-culture using enzyme-

120 linked immunosorbent assay (ELISA) confirmed antigen-specific organoid killing by the T

121 cells (Fig. 2e). In order to better follow the kinetics of the organoid killing, we applied a

122 fluorescent dye (NucRed Dead 647; Methods), which specifically stains apoptotic cells, and

123 performed live confocal imaging on the co-culture (Fig. 2f, Supplementary Movies 1 and 2).

124 We then quantified organoid killing by assessing co-localisation of NucRed Dead dye with

125 H2B-mNeonGreen (Methods). Significant co-localisation of both labels and, hence, organoid

126 killing, was only observed when peptide-pulsed HLA-A2$^+$ CRC organoids were co-cultured

127 with the respective peptide-specific T cells (Fig. 2g). Furthermore, T cells infiltrating into the

128 epithelium of the organoids could be readily detected in this co-culture condition (Fig. 2h).

129 Finally, we investigated whether using this co-culture system modulation of the immune

130 response to immunosuppressive tumours can be modelled. Indeed, addition of a blocking

131 antibody against PD-1 (αPD-1) enhanced tumour killing and IFN-γ production in PD-L1

132 expressing IFN-γ stimulated organoids (Fig. 2i,j). This was not observed when organoids were

133 not IFN-γ stimulated and, hence, did not express PD-1. In conclusion, T cells efficiently killed

134 co-cultured CRC organoids in an antigen-specific manner. In addition, T-cell inhibition and

135 subsequent relief of this inhibition using αPD-1 could be modelled.

4

Bar-Ephraim, Kretzschmar et al.

136

137 Here we demonstrate that epithelial organoids can be used to faithfully recapitulate the

138 interaction between tumour tissue and the immune system. Also, using our co-culture assay,

139 we set a first step in rebuilding the tumour microenvironment *in vitro*. Further addition of other

140 components of this microenvironment (such as fibroblasts, natural killer cells, myeloid-derived

141 suppressor cells, B cells) may shed light on the complex interactions between the different cell

142 types leading to immune evasion of the tumour. Lastly, in line with a recent publication

143 utilising cancer organoids as a scaffold for T-cell expansion[20], this co-culture system can be

144 used as a tool for drug-screens testing applicability of certain immunotherapies, for instance,

145 chimeric antigen receptor (CAR)- or TCR transgenic T cells, antibody-dependent cell-

146 mediated cytotoxicity (ADCC) or antibody-dependent cellular phagocytosis (ADCP) inducing

147 antibodies directed at the tumour, to different tumours and different patients.

148

149 **Methods**

150 *Human material and informed consent*

151 Colonic tissues (both normal colon and tumour tissue) were obtained from the Departments of

152 Surgery and Pathology of the Diakonessenhuis hospital, Utrecht, the Netherlands. All patients

153 included in this study were diagnosed with CRC. Informed consent was signed by all included

154 patients. Collection of tissue was approved by the medical ethical committee (METC) of the

155 Diakonessenhuis hospital, in agreement with the declaration of Helsinki and according to

156 Dutch and European Union legislation.

157

158 *Organoid generation and cultures*

159 Epithelial organoid lines were derived from healthy colon or tumor tissue as previously

160 described[12,21]. In brief, healthy colonic crypts were isolated by digestion of the colonic mucosa

161 in chelation solution (5.6 mM Na_2HPO_4, 8.0 mM KH_2PO_4, 96.2 mM NaCl, 1.6 mM KCl, 43.4

162 mM Sucrose, and 54.9 mM *D*-Sorbitol, Sigma) supplemented with dithiotreitol (0.5 mM,

163 Sigma) and EDTA (2 mM, in-house), for 30 minutes at 4°C. Colon crypts were subsequently

164 plated in basement membrane extract (BME; Cultrex PC BME RGF type 2, Amsbio) and

165 organoids were grown in human intestinal stem cell medium (HISC), which is composed of

166 Advanced Dulbecco's modified Eagle medium/F12 supplemented with

167 penicillin/streptomycin, 10 mM HEPES and Glutamax (all Gibco, Thermo Fisher Scientific)

168 with 50% Wnt3a conditioned medium (in-house), 20% R-Spondin1 conditioned medium (in-

169 house), 10% Noggin conditioned medium (in-house), 1 x B27, 1,25 mM n-acetyl cysteine, 10

Bar-Ephraim, Kretzschmar et al.

170   mM nicotinamide, 50 ng/mL human EGF, 10 nM Gastrin, 500 nM A83-01, 3 μM SB202190,

171   10 nM prostaglandine E2 and 100 μg/mL Primocin (Invivogen). Tumor specimens were

172   digested to single cells in collagenase II (1 mg/mL, Gibco, Thermo Scientific), supplemented

173   with hyaluronidase (10 μg/mL) and LY27632 (10 μM) for 30 minutes at 37°C while shaking.

174   Single tumor cells were plated in BME and organoids were cultured in HICS minus Wnt

175   conditioned medium and supplemented with 10 μM LY27632 at 37°C.

176

177   *Organoid transfection*

178   CRC organoids were dissociated into small clumps using TrypLE and then transduced with

179   H2B-mNeonGreen (pLV-H2B-mNeonGreen-ires-Puro), as previously described[22].

180

181   *T cells*

182   Generation of αβ T cells carrying a transgenic TCR recognizing an HLA-A2-restricted WT1-

183   derived peptide were described elsewhere[18]. Briefly, TCRα and β chains were cloned from

184   raised tetramer positive T cell clones. Subsequently, CD8$^+$ αβ TCR T cells were transduced

185   using retroviral supernatant from Phoenix-Ampho packaging cells that were transfected with

186   gag-pol, env, and pBullet retroviral constructs containing the cloned TCR genes.

187

188   *Organoid-T cell co-culture and live-cell imaging*

189   Organoids stably transfected with H2B-mNeonGreen were split and digested a 5 to 7 days prior

190   to co-culture and seeded at a density of 5000 cells per 10 μL of BME (25,000 cells per well in

191   a 12-well cell culture plate). Two days prior to co-culture, T cells were starved from IL-2. One

192   day prior to co-culture, organoids were stimulated with IFN-γ at indicated concentrations.

193

194   Prior to co-culturing, T cells were stained with Cell Proliferation Dye eFluor 450 (eBioscience)

195   according to the manufacturer's instructions. Organoids were pulsed with TCR-specific

196   peptide (ProImmune) for 2 hours at 37°C prior to co-culture. Organoids and T cells were

197   harvested and taken up in T cell medium, supplemented with 10% BME, 100 IU/mL IL-2 and

198   NucRed Dead 647 (Thermo Fischer). Where indicated, anti-PD1 blocking antibodies (2

199   μg/mL) were added to the co-culture. Cells were plated in glass-bottom 96-well plates and co-

200   cultures were imaged using an SP8X confocal microscope (Leica).

201

202   *Flow cytometry*

6

203   APC-labelled pentamers to the EBV-derived, HLA-2:02 restricted peptide FLYALALLL

204   (ProImmune) where used to sort pentamer+ CD8+ CD3+ T cells from PBMCs isolated from

205   buffycoats from healthy individuals. Cells were sorted as single cells into 96-well plates using

206   a BD FACS Aria (BD Biosciences) cytometer. For flow cytometry, the following antibodies

207   were used (all anti-human): CD8–PE (clone RPA-T8), CD45–PerCP-Cy5.5 (2D1), CD274

208   (PD-L1)–APC (MIH1) (all BD Biosciences), CD279 (PD-1)–PE (EH12.2H7, Biolegend),

209   HLA-A2–PE (BB7.2, Santa Cruz).

210

211   *Quantitative polymerase chain reaction (qPCR)*

212   For qPCR analysis, RNA was isolated from organoids using the RNAeasy kit (QIAGEN)

213   according to the manufacturer's protocol. PCR analysis was performed using the SYBR Green

214   Reagent (Biorad). PCR reactions were performed in duplicate with a standard curve for every

215   primer. Primers were designed using the NCBI primer design tool. Primers used in this study:

216   *GAPDH* forward (GTC GGA GTC AAC GGA TT), *GAPDH* reverse (AAG CTT CCC GTT

217   CTC AG), *HPRT* forward (GGC GTC GTG ATT AGT GAT), *HPRT* reverse (AGG GCT ACA

218   ATG TGA TGG), *CD274* forward (TGC AGG GCA TTC CAG AAA GAT), *CD274* reverse

219   (CCG TGA CAG TAA ATG CGT TCAG).

220

221   *Transcriptional profiling*

222   Microarray analysis of biobank organoids was performed as described elsewhere[12].

223

224   *Enzyme linked immunosorbent assays (ELISA)*

225   Culture supernatants were kept at −20°C and ELISA was performed for indicated cytokines

226   using ELISA MA Standard (Biolegend) according to manufacturer's protocol.

227

228   *Cell viability assay*

229   Cell viability after co-cultures was assessed using CellTiter-Glo Luminescent cell viability

230   assay (Promega), according to manufacturer's protocol.

231

232   *Image analysis*

233   Image analysis was done using Imaris software package (Bitplane). In brief, threshold for

234   positive staining was set on negative controls. A co-localization channel was made for H2B-

235   neon and NucRed Dead 647 signals. Cell death was quantified as percentage of H2B-

236   mNeonGreen+ voxels co-localising with NucRed Dead signal.

Bar-Ephraim, Kretzschmar et al.

237

Bioinformatics analysis

239 Bioinformatics analysis of normalised gene-expression data from microarray experiments[12]
240 was performed using standard packages (*i.e.* gplots) in R version 3.4.0 (R Foundation,
241 https://www.r-project.org) and RStudio version 1.0.143 (https://www.rstudio.com).

242

Statistical analysis

244 All experiments were repeated at least three times unless otherwise indicated. All data were
245 shown as mean ± SEM. Statistical significance was analysed by either ANOVA or two-tailed
246 Student's *t*-test using either Graphpad Prism 6 or Microsoft Excel 2010.

247

References

249 1.   Ferlay, J. *et al.* GLOBOCAN 2012 v1.0, Cancer Incidence and Mortality Worldwide:
250   IARC CancerBase No. 11. *International Agency for Research on Cancer* (2013).

251 2.   Markowitz, S. D., Dawson, D. M., Willis, J. & Willson, J. K. Focus on colon cancer.
252   *Cancer Cell* **1**, 233-236 (2002).

253 3.   Vries, R. G., Huch, M. & Clevers, H. Stem cells and cancer of the stomach and intestine.
254   *Mol Oncol* **4**, 373-384, doi:10.1016/j.molonc.2010.05.001 (2010).

255 4.   Markowitz, S. D. & Bertagnolli, M. M. Molecular origins of cancer: Molecular basis
256   of colorectal cancer. *N Engl J Med* **361**, 2449-2460, doi:10.1056/NEJMra0804588
257   (2009).

258 5.   Hanahan, D. & Weinberg, R. A. Hallmarks of cancer: the next generation. *Cell* **144**,
259   646-674, doi:10.1016/j.cell.2011.02.013 (2011).

260 6.   Junttila, M. R. & de Sauvage, F. J. Influence of tumour micro-environment
261   heterogeneity on therapeutic response. *Nature* **501**, 346-354, doi:10.1038/nature12626
262   (2013).

263 7.   Gajewski, T. F., Schreiber, H. & Fu, Y. X. Innate and adaptive immune cells in the
264   tumor microenvironment. *Nat Immunol* **14**, 1014-1022, doi:10.1038/ni.2703 (2013).

265 8.   Dunn, G. P., Koebel, C. M. & Schreiber, R. D. Interferons, immunity and cancer
266   immunoediting. *Nat Rev Immunol* **6**, 836-848, doi:10.1038/nri1961 (2006).

267 9.   Zitvogel, L., Galluzzi, L., Smyth, M. J. & Kroemer, G. Mechanism of action of
268   conventional and targeted anticancer therapies: reinstating immunosurveillance.
269   *Immunity* **39**, 74-88, doi:10.1016/j.immuni.2013.06.014 (2013).

270   10.   Kretzschmar, K. & Clevers, H. Organoids: Modeling Development and the Stem Cell

271   Niche in a Dish. *Dev Cell* **38**, 590-600, doi:10.1016/j.devcel.2016.08.014 (2016).

272   11.   Drost, J. & Clevers, H. Organoids in cancer research. *Nat Rev Cancer* **18**, 407-418,

273   doi:10.1038/s41568-018-0007-6 (2018).

274   12.   van de Wetering, M. *et al.* Prospective derivation of a living organoid biobank of

275   colorectal cancer patients. *Cell* **161**, 933-945, doi:10.1016/j.cell.2015.03.053 (2015).

276   13.   Leone, P. *et al.* MHC class I antigen processing and presenting machinery:

277   organization, function, and defects in tumor cells. *J Natl Cancer Inst* **105**, 1172-1187,

278   doi:10.1093/jnci/djt184 (2013).

279   14.   Fearon, E. R. & Vogelstein, B. A genetic model for colorectal tumorigenesis. *Cell* **61**,

280   759-767 (1990).

281   15.   Drost, J. *et al.* Sequential cancer mutations in cultured human intestinal stem cells.

282   *Nature* **521**, 43-47, doi:10.1038/nature14415 (2015).

283   16.   Fumagalli, A. *et al.* Genetic dissection of colorectal cancer progression by orthotopic

284   transplantation of engineered cancer organoids. *Proc Natl Acad Sci U S A* **114**, E2357-

285   E2364, doi:10.1073/pnas.1701219114 (2017).

286   17.   Kryczek, I. *et al.* Cutting edge: IFN-gamma enables APC to promote memory Th17

287   and abate Th1 cell development. *J Immunol* **181**, 5842-5846 (2008).

288   18.   Kuball, J. *et al.* Facilitating matched pairing and expression of TCR chains introduced

289   into human T cells. *Blood* **109**, 2331-2338, doi:10.1182/blood-2006-05-023069 (2007).

290   19.   Sebestyen, Z. *et al.* RhoB Mediates Phosphoantigen Recognition by Vgamma9Vdelta2

291   T Cell Receptor. *Cell Rep* **15**, 1973-1985, doi:10.1016/j.celrep.2016.04.081 (2016).

292   20.   Dijkstra, K. K. *et al.* Generation of Tumor-Reactive T Cells by Co-culture of Peripheral

293   Blood Lymphocytes and Tumor Organoids. *Cell* **174**, 1586-1598 e1512,

294   doi:10.1016/j.cell.2018.07.009 (2018).

295   21.   Sato, T. *et al.* Long-term expansion of epithelial organoids from human colon,

296   adenoma, adenocarcinoma, and Barrett's epithelium. *Gastroenterology* **141**, 1762-

297   1772, doi:10.1053/j.gastro.2011.07.050 (2011).

298   22.   Bolhaqueiro, A. C. F. *et al.* Live imaging of cell division in 3D stem-cell organoid

299   cultures. *Methods in cell biology* **145**, 91-106, doi:10.1016/bs.mcb.2018.03.016 (2018).

300

301   **Acknowledgements**

Bar-Ephraim, Kretzschmar et al.

312

313   Author contributions

314   Y.B.E. and K.K. designed, performed and analysed the experiments and wrote the manuscript.
315   Y.B.E. performed image analysis. K.K. performed bioinformatics analysis. P.A., E.d.J. and
316   K.E.B. assisted with experiments. J.D. generated cancer gene-mutant organoid lines. J.v.G.
317   isolated tumour and normal tissue from resected material. A.P. and N.S. performed surgery.
318   I.J.G., Z.S. and J.K. provided WT1 peptide and WT1 peptide-specific transgenic TCR $\alpha\beta$ T
319   cells. R.G.J.V. organised tissue collection. K.K. and H.C. acquired funding. H.C. supervised
320   the project and wrote the manuscript. All of the authors commented on the manuscript.

321

Bar-Ephraim, Kretzschmar et al.
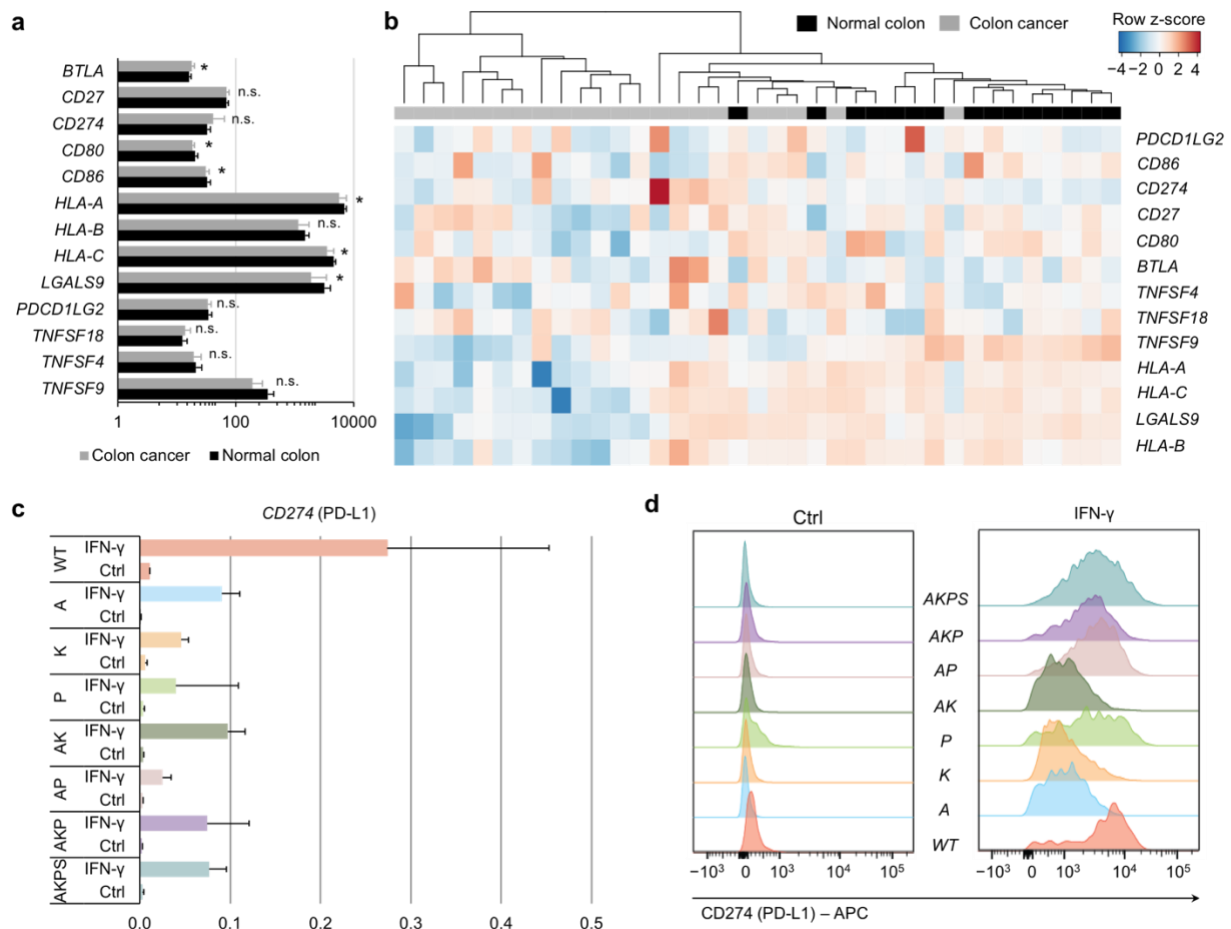
Fig. 1 | CRC organoids express immunomodulatory molecules. a,**b**, Normal colon and CRC organoid lines were generated in a patient-specific manner and RNA was extracted and analysed using Affymetrix single transcript microarrays. Average gene expression of different immunomodulators in normal colon and CRC organoid lines; n.s., non-significant; *, $p < 0.05$ (**a**). Hierarchical clustering of the individual normal colon and CRC organoid lines in the 'living biobank' displaying gene expression of selected immunomodulators. Color gradients represent z valued of each row (gene transcripts). **c-d**, Human colon organoid lines genetically engineered to carry one or more mutations found in CRCs. Expression levels of CD274 (PD-L1) in organoid lines (n = 2) at steady state (Ctrl) and upon stimulation with 20 ng/mL recombinant human IFN-γ assessed by quantitative PCR (**c**) and flow cytometry (**d**). A, $APC^{KO/KO}$; N.D., not detected; K, $KRAS^{G12D/+}$: P, $P53^{KO/KO}$; S, $SMAD4^{KO/KO}$, WT, wild-type.

11

Bar-Ephraim, Kretzschmar et al.
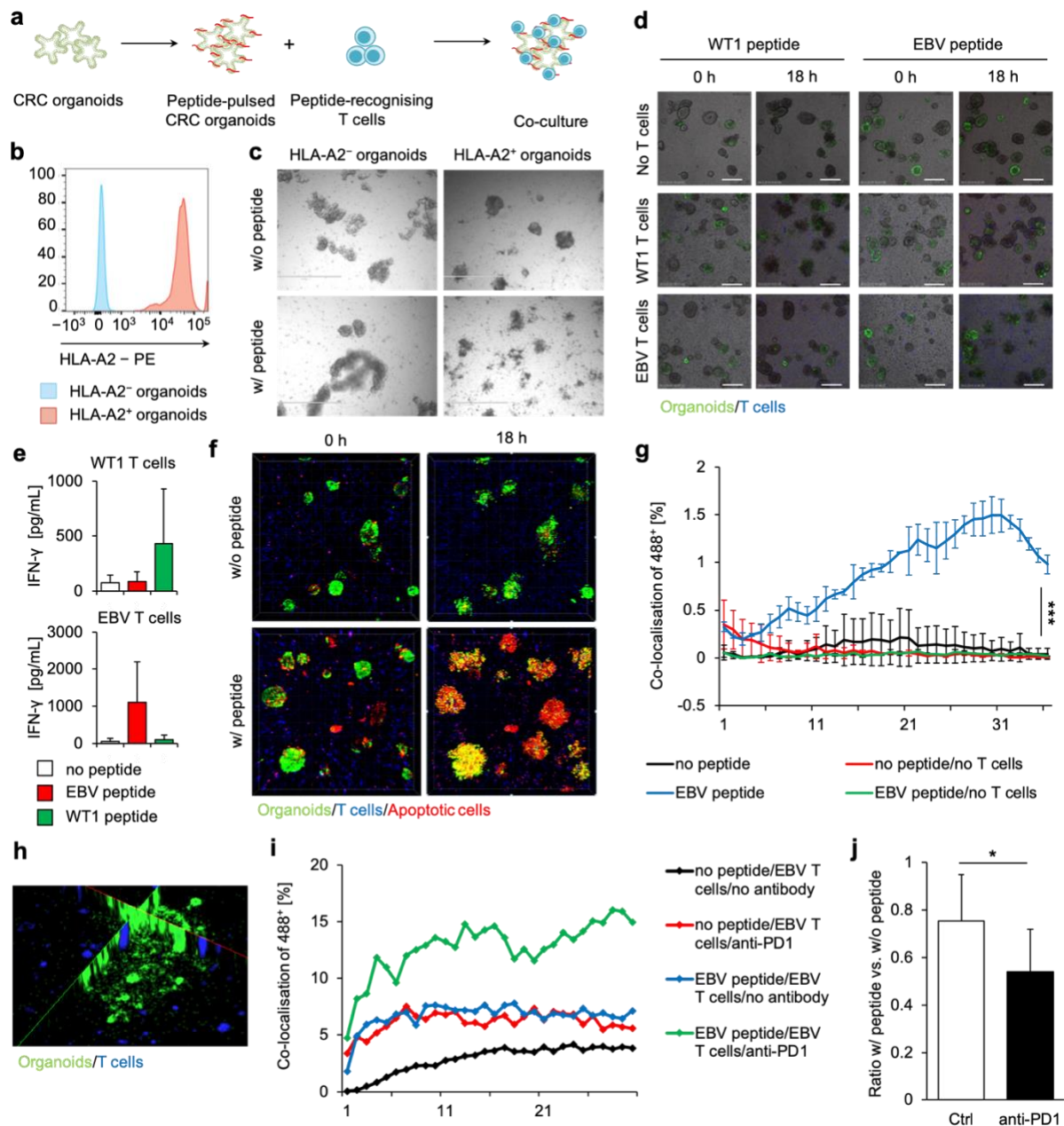
Fig. 2 | CRC organoids as tools for assessment of antigen specific killing by CD8+ T cells.
a, Experimental scheme. **b**, Flow cytometry analysis of HLA-A2 expression in cloned HLA-A2+ and HLA-A2− lines. **c**, Brightfield images of CRC organoids co-cultured with WT1 peptide-specific T-cell receptor-specific transgenic T cells for 48 hours; scale bars: 1 mm. **d**, Images showing peptide-pulsed HLA-A2+ CRC organoids at the beginning and end of co-culture with indicated peptide-specific T cells; scale bars: 70 µm. **e**, IFN-γ production by WT1 (top) and EBV (bottom) peptide-specific T cells as measured by ELISA of supernatants collected after 18-hour co-culture with HLA-A2+ CRC organoids pulsed with indicated peptides. **f**, Live-cell imaging stills of an 18-hour co-culture experiment with EBV peptide-

Bar-Ephraim, Kretzschmar et al.

347 pulsed HLA-A2$^+$ CRC organoids co-cultured with an EBV-specific T-cell clone. **g**,

348 Quantification of CRC organoid killing by specific T cells. Graphs are representative of

349 multiple repeated experiments with either EBV peptide and EBV T-cell- or WT1 peptide and

350 WT1 T-cell co-cultures. **h**, Representative projection image of T cells (blue) infiltrating a

351 peptide-pulsed CRC organoid as recorded during the live-cell imaging experiments. **i**,

352 Quantification of killing of IFN-γ treated CRC organoids by specific T cells in either presence

353 or absence of a blocking antibody against PD-1. Graphs are representative of multiple repeated

354 experiments with either EBV peptide and EBV T-cell- or WT1 peptide and WT1 T-cell co-

355 cultures. **j**, Quantification cell viability after 18 hours co-cultures of either peptide pulsed or

356 non-pulsed HLA-A2$^+$ organoids with antigen specific T cells. Graphs represent ratio between

357 peptide-pulsed and non-peptide pulsed conditions.

358